

We are IntechOpen, the world's leading publisher of Open Access books Built by scientists, for scientists

4,800

Open access books available

122,000

International authors and editors

135M

Downloads

Our authors are among the

154

Countries delivered to

TOP 1%

most cited scientists

12.2%

Contributors from top 500 universities



WEB OF SCIENCE™

Selection of our books indexed in the Book Citation Index
in Web of Science™ Core Collection (BKCI)

Interested in publishing with us?
Contact book.department@intechopen.com

Numbers displayed above are based on latest data collected.
For more information visit www.intechopen.com



Redox Potentials as Reactivity Descriptors in Electrochemistry

José H. Zagal, Ingrid Ponce and Ruben Oñate

Abstract

A redox catalyst can be present in the solution phase or immobilized on the electrode surface. When the catalyst is present in the solution phase the process can proceed via inner- (with bond formation, chemical catalysis) or outer-sphere mechanisms (without bond formation, redox catalysis). For the latter, $\log k$ is linearly proportional to the redox potential of the catalysts, E° . In contrast, for inner-sphere catalyst, the values of k are much higher than those predicted by the redox potential of the catalyst. The behaviour of these catalysts when they are confined on the electrode surface is completely different. They all seem to work as inner-sphere catalysts where a crucial step is the formation of a bond between the active site and the target molecule. Plots of $(\log i)_E$ versus E° give linear or volcano correlations. What is interesting in these volcano correlations is that the falling region corresponding to strong adsorption of intermediates to the active sites is not necessarily attributed to a gradual surface occupation of active sites by intermediates (Langmuir isotherm) but rather to a gradual decrease in the amount of M(II) active sites which are transformed into M(III)OH inactive sites due to the applied potential.

Keywords: redox potential, reactivity descriptors, redox catalysis, chemical catalysis, linear free-energy correlations, volcano correlations

1. Introduction

Predicting the rate of chemical processes on the basis of thermodynamic information is of fundamental importance in all areas of chemistry including biochemistry, coordination chemistry and especially electrochemistry [1]. Correlations do exist between the Gibbs free-energy for one series of reactions and logarithm of the reaction rate constant for a related series of reactions. These relations are known as linear free-energy relationships (LFER) [1]. For example, the Brønsted catalysis equation describes the relationship between the ionization constant of a series of catalysts and the reaction rate constant for a reaction on which the catalyst operates. The Hammett equation predicts the equilibrium constant or reaction rate constant of a reaction from a substituent constant and a reaction type constant. The Edwards equation relates the nucleophilic power to polarizability and basicity. The Marcus equation is an example of a quadratic free-energy relationship (QFER) that applies to electron transfer (ET) reactions where the activation energy is given by the inner and outer reorganizational energies. In the case of electrochemical reactions, the

thermodynamics can be provided by the electrode potential or by the redox potential of a mediator or both [1].

The slope of the linear free-energy correlations reflects the sensitivity of rate constant to structural changes in a family of similar reactions. For organic reactions this slope resembles the definition of the parameter σ in Hammett correlations. It is interesting to mention that already in 1932 Frumkin stated [2] that at different electrode potentials, an electrochemical reaction is equivalent to a series of similar reactions differing only by the magnitude of ΔG° , where ΔG° is equal to $-nF\Delta E^\circ$ [3], n is the number of electrons exchanged in the complete reaction and F is the Faraday constant. In this case the role of substituents for changing the driving force is played by the potential of the electrode applied by an external source. The most common linear free-energy relationship in electrochemistry is the Tafel plot [4, 5], where $(\log i)$ is plotted versus the potential of the electrode. This linear correlation is observed in the absence of mass transport limitations. If i is a kinetic current density, $\log i$ is proportional to $\log k$ (k is the rate constant), and the potential of the electrode is proportional to ΔG° . As discussed further down, these correlations are not always linear in electron transfer processes in the homogenous phase or at electrode interfaces. In this chapter we will focus our attention of the correlations between the redox potential, a thermodynamic parameter of the catalyst and its catalytic activity. As we will discuss, these correlations are sometimes linear, and on other occasions they can have the shape of a volcano.

2. Catalytic effects in electrochemistry

A redox catalyst is a molecule that has an atom with two oxidation states that are kinetically more favorable than the oxidation states of the reactants and products upon which the catalyst is operating. In general, the most common active site is a metal that can be an atom that is coordinative unsaturated and is active for binding extraplanar ligands such as the reacting molecules [1]. The catalyst can be present in the solution phase or immobilized on the electrode surface. When the catalysts are present in the solution phase, the process can proceed via inner- or outer-sphere mechanisms [1]. For the latter, $\log k$ is linearly proportional to E° , whereas for inner-sphere catalyst, the values of k are much higher than those predicted by the formal potential of the catalyst. The behaviour of these catalysts when they are confined on the electrode surface is completely different. They all work as inner-sphere catalysts where a crucial step is the formation of a bond between the active site and the target molecule. Plots of $(\log i)_E$ versus E° give volcano plots.

2.1 Redox catalysis and chemical catalysis

Metal, metal alloys and metal oxides have been studied extensively in the literature as catalysts for many reactions since the beginnings of electrochemistry. For example, the hydrogen evolution reaction (HER) was studied by Tafel [4], and he derived from his studies his well-known equation. In contrast, molecular catalysts have only been studied more intensively rather recently than the long history of fundamental and applied work using metals and alloys. It is important to point out that the electronic structure of metal electrodes is described using d -band theories where electronic levels form a continuum in the valence band. In contrast, molecular catalysts have discrete energy levels like any isolated chemical molecule or isolated atom. It is interesting then to correlate the electronic properties and energy levels of molecular catalysts with their catalytic activity for any reaction [6].

As mentioned above, a redox molecular catalyst is a species that can present at least two oxidation states that are kinetically much more favorable than the oxidation states of the reactants and products that the catalyst is promoting. Some electrochemical reactions involving reactants in the solution phase proceed at reasonable rates at potentials that are close to the equilibrium potential of the reaction, i.e. they require a rather low overpotential for the process to proceed at measurable rates. The kinetics of these reactions are then rather fast. A typical example is HER occurring on a Pt electrode [1]. However, many electrochemical reactions of interest usually require the transfer of more than one electron, each electron transfer step representing an energy barrier. The slow step, which is the rate-determining step, can be accelerated by the action of electrocatalysts mainly in two ways (some of them are illustrated in **Figure 1**):

- i. The catalyst is in the solution phase, and the electrode serves only as a sink or source of electrons. The electrode regenerates the active form of the catalyst continuously which interacts with the target molecule in the homogeneous phase.
- ii. The process is heterogeneous, and the catalyst can be the electrode surface itself (e.g. *d*-type noble metals like Pt, Pd, etc.) or a molecular catalyst confined on a rather inert electrode surface (i.e. for so-called modified electrodes). In the case of a molecular catalyst attached to the electrode surface, the electrode also regenerates the active form of the catalyst continuously.

2.1.1 Case (i): the catalyst is present in the solution phase

In case (i), the homogeneous catalytic process can proceed via two different pathways: via outer-sphere and inner-sphere processes [7].

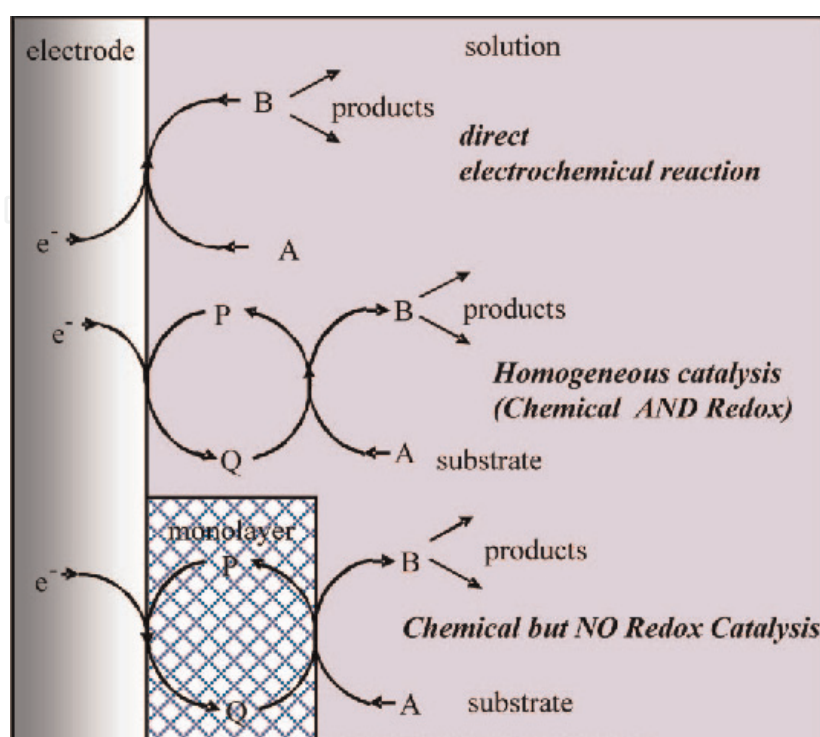
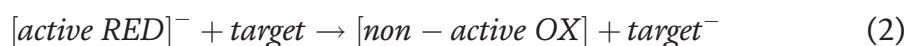


Figure 1. Different reactions schemes for catalytic processes in electrochemistry as described by Savéant [7] (reproduced by permission John Wiley & son).

(ia) For the case of an outer-sphere reaction, the process has been termed “redox catalysis”, and the active form of the catalysts is present in a given oxidation state. The catalyst oxidation state changes upon interacting with the target molecule, and the active state is continuously regenerated at the electrode surface. The catalyst and the reactant only collide in the homogeneous phase without forming a bond. The catalyst recuperates its initial oxidation state at the electrode surface as illustrated in **Figure 1**. The catalysis in this case lowers the overpotential of the overall reaction by acting in a three-dimensional dispersion. The redox potential of the catalyst contributes to the driving force of the reaction, not the potential of the electrode, which only serves to regenerate the active form of the catalyst at the interface (no reaction takes place directly between the electrode and the reactants [7]).

(ib) For the case of an “inner sphere” process, the process has been termed “chemical catalysis” and involves the temporary formation of an adduct between the mediator and the reactant. The bond formed between the reactant and the catalyst is broken after the exchange of electrons to form intermediates and products. This regenerates the catalysts that recuperate its initial oxidation state at the electrode [7].

If we take as an example a reduction reaction mediated by catalysts dissolved in the solution phase, on thermodynamic grounds one would expect that the more negative the formal potential of the mediator (more powerful reductant), the higher its reactivity for the oxidation of the target, according to the reaction scheme below, where step in Eq. (3) is rate-determining and the first step, Eq. (1), is the electrogeneration of the catalyst in its active form:



According to this reaction scheme and assuming that step 3, Eq. (3), is rate controlling, the rate of the reaction is:

$$\frac{-d[\text{target}]}{dt} = \frac{kK[\text{target}][\text{non} - \text{activeOX}]}{[\text{activeRED}]^-} = k[\text{target}] * 10^{(E-E^{\circ})/0.059} \quad (4)$$

Savéant et al. [7–11] carried out a series of studies using different redox catalysts for the homogeneous reduction of alkyl halides and vicinal halides to alkenes. They identified two types of catalytic systems: outer-sphere and inner-sphere redox catalysts. **Figures 2** and **3** show a linear correlation between the E° formal potential of the catalysts and $\log k$ for outer-sphere catalysts. Inner-sphere catalysts fall out for the linear correlation. In the latter, the catalytic effect originates from the formation of an adduct between the reacting molecule and the catalyst, which lowers the activation energy of the process. The reaction studied involved the rupture of a bond so Marcus theory cannot be applied but rather a modified version proposed by Savéant that describes a Morse curve rather than a parabola for the reaction products [11]. In the latter, the catalytic effect rises from the formation of an adduct between the reacting molecule and the catalyst, which lowers the activation energy of the process. For inner-sphere processes where the redox catalysts are in the homogeneous phase, there is no clear dependence of the rate of the process of the redox potential of the catalyst. The inner-sphere process has lower activation energy than the outer-sphere pathway. If both pathways are available, the inner-sphere process is preferred.

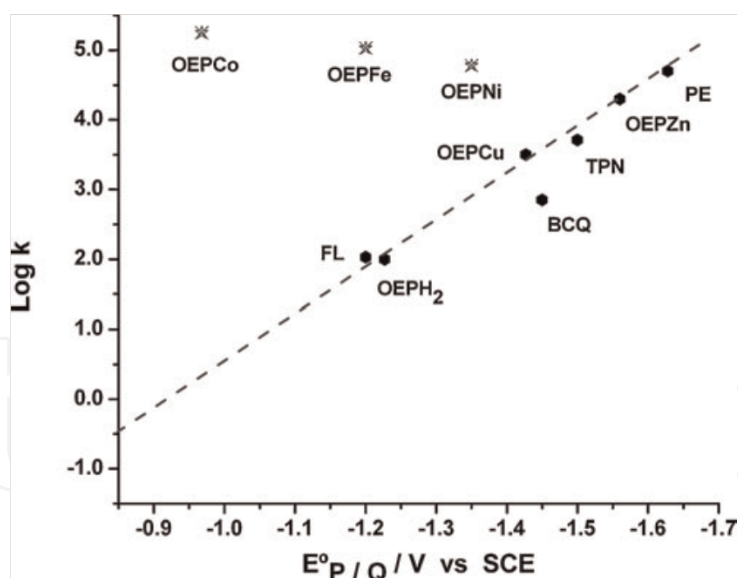


Figure 2. Dependence of $\log k$ versus the redox potential of the catalyst for the reduction of *trans*-1,2 dibromocyclohexane by aromatic radicals and by reduced metalloporphyrins from Lexa et al. [11] (reproduced by permission of the American Chemical Society).

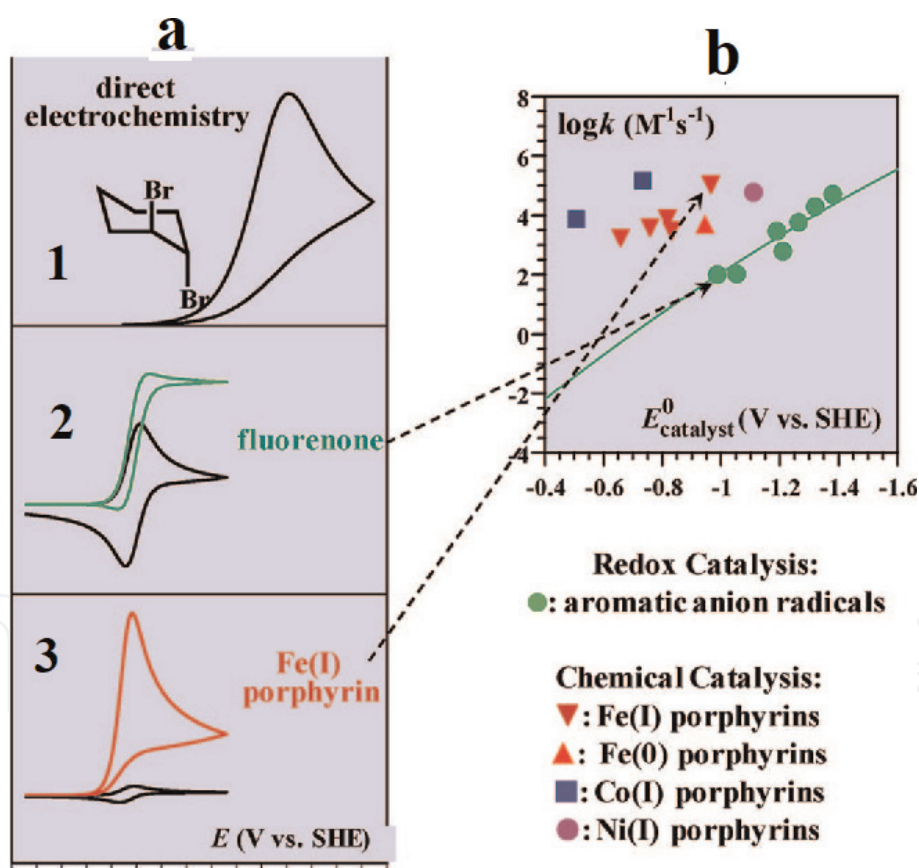


Figure 3. Homogeneous redox and chemical catalysis of *trans*-1,2 dibromocyclohexane. (a₁) Cyclic voltammogram in DMF of direct electrochemical reduction on glassy carbon, (a₂) redox catalysis of fluorenone and (a₃) chemical catalysis promoted by iron(I) porphyrin. (b) Rate constant versus the standard redox potential of the catalyst (taken from Savéant [7]). Reproduced by permission John Wiley & son).

2.1.2 Electrocatalysis by redox mediators, chemical catalysis and oxygen reduction

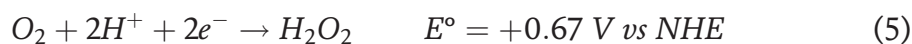
Electrodes modified with macrocyclic metal complexes that exhibit fast reversible redox processes centred on the metal have received considerable attention in

the literature because of the applications in electrocatalysts and also as electrochemical sensors [12–14]. A very important area that has been investigated by many authors for decades is the oxygen reduction reaction (ORR). The ORR is a very important reaction indeed as it is involved in energy conversion processes (fuel cells, air batteries) in metallic corrosion etc., without considering important biological processes as the respiration chain [15]. The complete reduction of O₂ in aqueous media requires the presence of catalysts and involves the transfer of four electrons and the splitting of the O–O bond. This reaction delivers the most energy in a fuel cell and in living systems. However, in electrochemistry rather few electrode materials promote the four-electron reduction of O₂.

The ORR process is a multielectron reaction in aqueous media that occurs via two main pathways: one involving two electrons to give peroxide and the direct four-electron pathway to give water. The four-electron process involves the rupture of the O–O bond [16]. The nature of the electrode surface strongly influences the preferred pathway. Most electrode materials catalyse the reaction only via two electrons to form peroxide:

Pathways for ORR.

In acid media:



In alkaline media:



Peroxide formation during O₂ reduction can be followed by its reduction:



or by its chemical decomposition:



Direct four-electron reduction pathway.

In acid:



In alkaline:



In strongly alkaline solutions or in organic solvents, O₂ is reduced via the transfer of a single electron to give superoxide ion. This process is outer-sphere:



The O₂ four-electron reduction reaction is thermodynamically spontaneous in O₂/H₂ fuel cells, but its kinetics are slow on most electrode materials. The sluggishness of the reaction kinetics can be attributed to the transfer of four electrons involving the formation of bonds between intermediates and the active sites. The best catalytic materials for the four-electron ORR contain Platinum. The high cost of this metal is one of the limitations for the widespread use of fuel cells. Several

authors have faced the challenge of preparing catalytic materials for oxygen reduction that do not involve precious metals like Platinum and its alloys. This probably started with the seminal work of Jasinski [17] that reported that cobalt phthalocyanine (CoPc) exhibited catalytic activity for the ORR. This discovery triggered the research on metal macrocyclic MN₄ complexes as potential catalysts for ORR.

Figure 4 shows the molecular structures of the most common macrocyclic complexes investigated as catalysts for ORR. However, some MN₄ electrodes containing these complexes are not stable in the corrosive environment of a fuel cell after long operating conditions. For this reason, a new research started, on pyrolysed MN₄ complexes [18]. Heat treatment at different temperatures increases both activity and stability, and this has been demonstrated by several authors. It was also found that MN₄ or MN_x pyrolysed catalytic materials can be obtained without using MN₄ complexes as a starting ingredient, but rather using metal salts and N-containing organic compounds.

In this chapter, we will discuss the different reactivity predictors that serve as guidelines for the synthesis of more active catalysts [6, 12, 14, 16, 19–22] but with emphasis on the redox potential of the catalyst. There are several reactivity predictors for MN₄ macrocyclic complexes that have been described in the literature: (i) the *d*-level populations in the central metal, (ii) the donor-acceptor intermolecular hardness, (iii) the M-O₂ binding energy and (iv) the M⁺ⁿ/M⁺⁽ⁿ⁻¹⁾ redox potential. We will discuss predictors (i) and (iii)–(iv), especially the last two, the M-O₂ binding energy and the redox potential of the catalysts, as they seem to be related to each other. One rather simple reactivity predictor is the number of *d*-electrons when comparing the activities of a family of similar macrocyclic metal complexes. For example, when comparing the activities of metal phthalocyanines (MPcs), a plot of *E* at constant current versus the number of *d*-electrons gives a

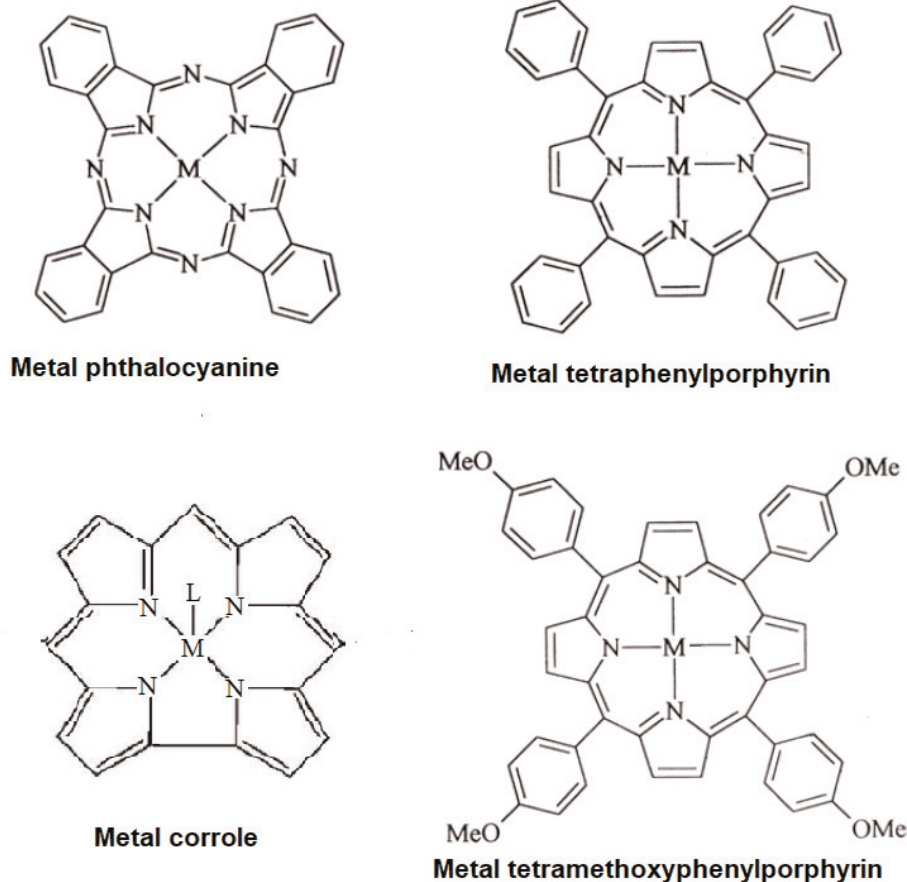


Figure 4. Structure of several unsubstituted and substituted metal phthalocyanines, metal porphyrins and a metal corrole.

parabolic correlation with FePc showing the highest activity with 6 *d*-electrons. When metal porphyrins (MPs) are compared, the highest activity is exhibited by CoPs with 7 *d*-electrons. These results are illustrated in **Figure 5**. These results indicate that highest activity is achieved by complexes with nearly half-filled *d*-orbitals. However, it is important to point out that those metals with low and or partially filled *d*-orbitals exhibit reversible redox processes located on the metal centre. This is true for Cr, Mn, Fe and Co macrocyclic complexes. The frontier orbitals of these complexes have *d*-character and have the proper symmetry to bind an extraplanar ligand like O₂. On the other hand, Ni, Cu and Zn complexes exhibit no redox process centred on the metal and redox processes involve the ligand. These complexes show less catalytic activity for ORR and other reactions. We will discuss further down the important role that the redox potential plays in dictating the catalytic activity. As a graphical example, **Figure 6** illustrates electron tunneling microscopy images obtained with CoPc and CuPc by two different authors [12, 19]. It is clear that CoPc shows an electron-rich zone on the central metal in contrast to CuPc. This is corroborated in the same **Figure 6C** by frontier orbital profiles

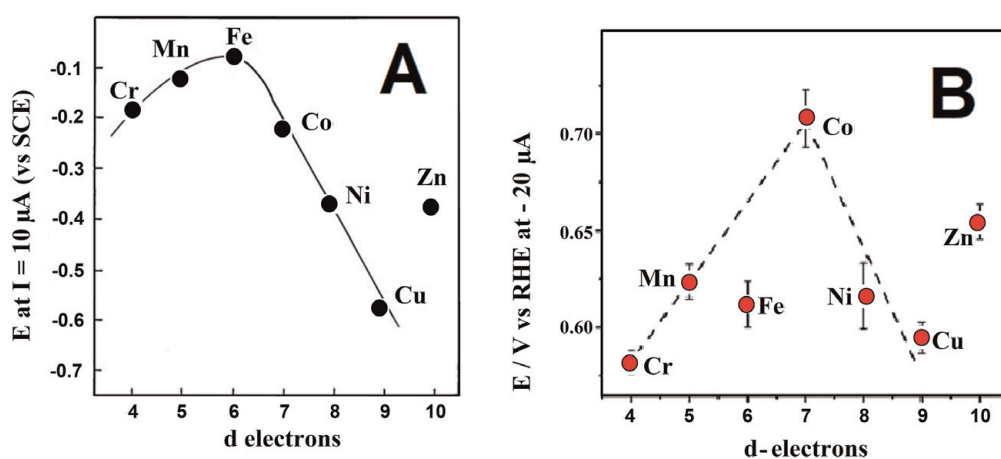


Figure 5. Correlation between electrocatalytic activity (as potential at constant current) versus the number of *d*-electrons for ORR in alkaline media on metallo-phthalocyanines (A) and metal porphyrins (B) (data on MPcs from [12] and MPcs from [19]).

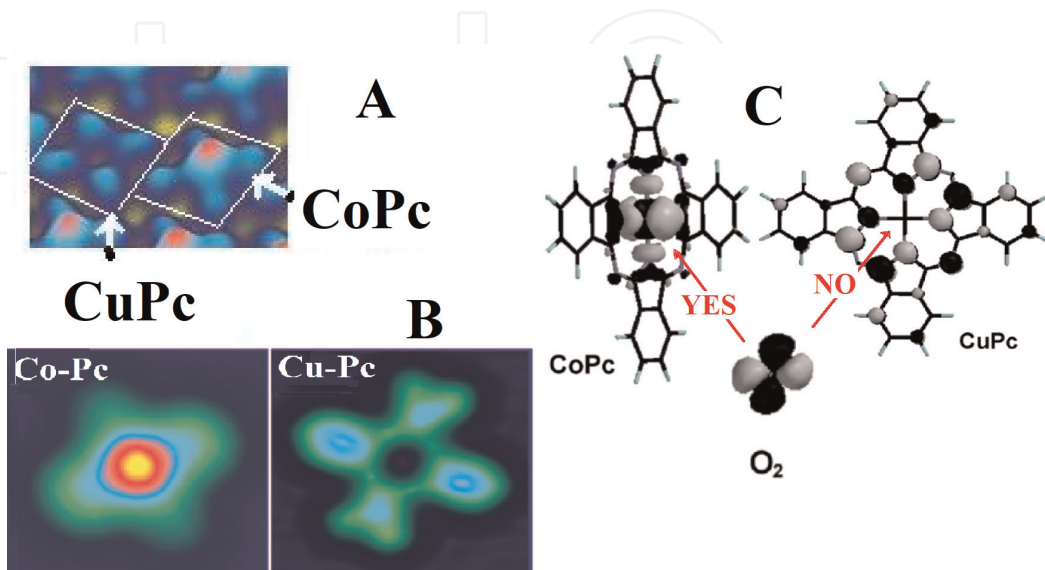


Figure 6. (A and B) tunnel microscopy images of CuPc (inactive) and CoPc (active) adsorbed on Au (adapted from [20, 21]). (C) theoretical profiles of frontier orbitals of CoPc and CuPc (taken from [22] with permission from Elsevier).

obtained theoretically that show that CoPc exhibits a prominent d -orbital that can bind O_2 in contrast again to CuPc. These images are in agreement with the reactivity trends shown in **Figure 5A**.

Figure 7 illustrates a correlation of catalytic activity as $(\log i)_E$ for ORR at constant potential versus the M(III)/(II) redox potential of the catalyst; the data was obtained in acid solution (8 M H_2SO_4) [23]. It is clear from this figure that the activity increases almost linearly with the redox potential of the catalyst up to a point and then decreases. A maximum activity is observed for octaethyl CoPs (see CoOEP in **Figure 7**). It is interesting that Fe complexes appear on one side of the volcano and Co complexes on the other side. These volcano-shaped correlations are very common in electrocatalysis and heterogeneous catalysis, but instead of the redox potential a parameter is used that describes the degree of interaction of O_2 with the active site. In recent work the M- O_2 binding energy is used [6], and this parameter is the most common reactivity descriptor. The data in **Figure 7** strongly suggests that the redox potential of the catalyst is a reactivity descriptor and then should be related to the M- O_2 energy.

Figure 8 clearly shows that there is a direct correlation between the M(III)/(II) redox potential of the catalyst and the M- O_2 binding energy, for redox data obtained in alkaline media [6]. The data in **Figure 8** indicates that the M- O_2 binding is a reactivity descriptor for ORR catalysed by MN4 macrocyclic complexes as is well established for metal electrodes [24]. Strong binding catalysts appear on the left side of the volcano, and weak binding catalysts appear on the right-hand side of the correlation, illustrating that these catalysts follow the Sabatier principle that for achieving the highest catalytic activity, the binding needs to be not too strong and not too weak. The volcano correlation illustrated in **Figure 8** bears a strong resemblance with similar volcano correlations obtained for ORR catalysed by pure metals [24]. For both MN4 complexes and pure metals, strong binding catalysts promote the four-electron reduction of O_2 to water or OH^- , whereas weak binding catalysts only promote the two-electron reduction to hydrogen peroxide.

Figure 9 illustrates the potentiodynamic response of CoPc/OPG and FePc/OPG, where OPG is ordinary pyrolytic graphite electrode, and also the reduction wave for

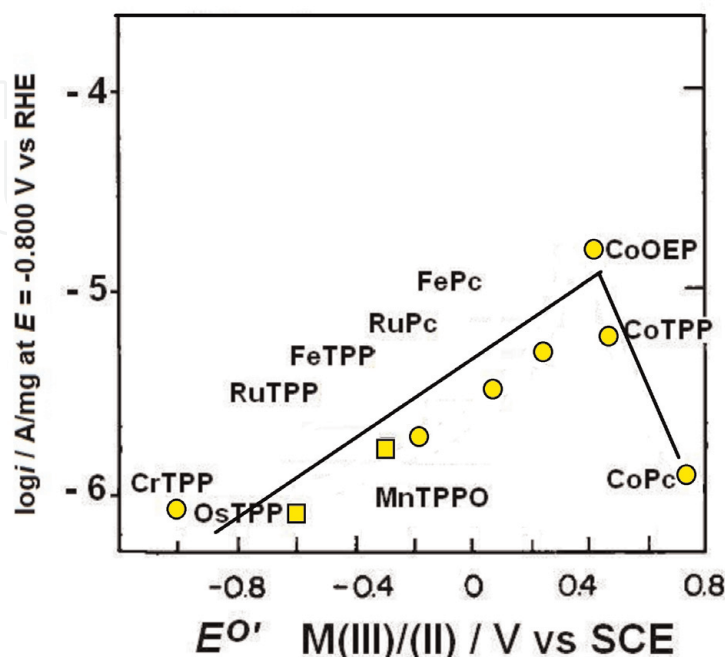


Figure 7. Illustration of volcano correlations of catalytic activity as $(\log i)_E$ for ORR at constant potential versus the M(III)/(II) redox potential of the catalyst. The data was obtained in acid solution (8 M H_2SO_4) [23].

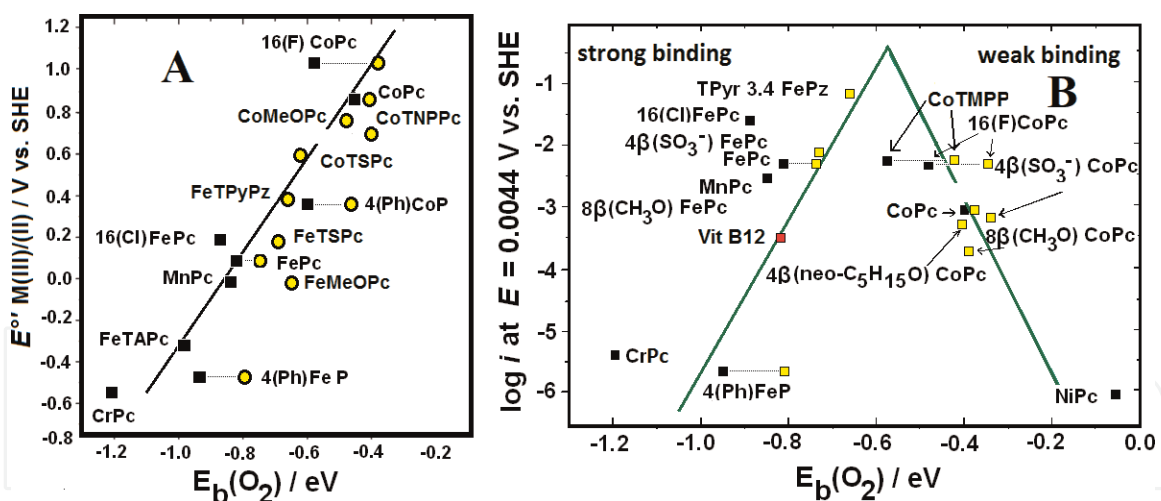


Figure 8.

(A) Correlation of electrocatalytic versus M(III)/(II) redox potential of the MN₄ complexes and (B) versus the M-O₂ binding energy to the metal center in the MN₄ complex (ref.[6] and references there in).

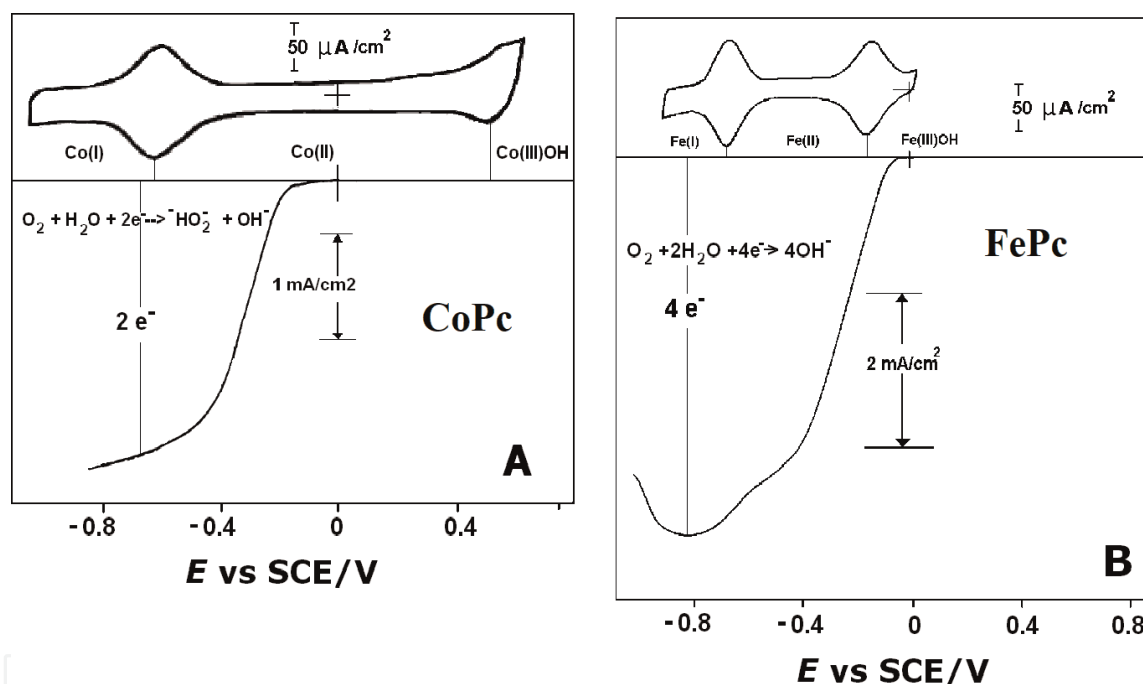


Figure 9.

(A) Cyclic voltammogram obtained in 0.1 M NaOH with an ordinary pyrolytic graphite (OPG) disk electrode modified with a monolayer of CoPc in the absence of O₂. The bottom of that figure shows a polarization curve obtained with the same electrode, in the presence of O₂ (saturated) and with rotation of 1000 rpm. (B) Analogous to (A) but with the OPG electrode modified with FePc [25].

ORR obtained on rotating OPG disk modified with monolayers of CoPc or FePc. Both complexes exhibit M(II)/(I) and M(III)/(II) reversible redox couples in the potential range examined. However, there are some striking differences in the response of these two complexes: first, the Co(II)/(I) and Co(III)/(II) redox couples appear much more separated for CoPc than similar processes occurring on FePc. For CoPc the onset for ORR appears at potentials between the Co(II)/(I) and Co(III)/(II) transitions, and the onset is well removed in the positive direction from the Co(III)/(II) redox potential, whereas for FePc, the onset for ORR appears at a potential close and more positive than the Fe(III)/(II). In this case ORR starts at potentials where the surface coverage by Fe(II) active sites is potential-dependent, and this coverage gradually increases as the potential is scanned to more negative potentials [25]. **Figure 10** illustrates the potential dependence of the coverage of the surface by

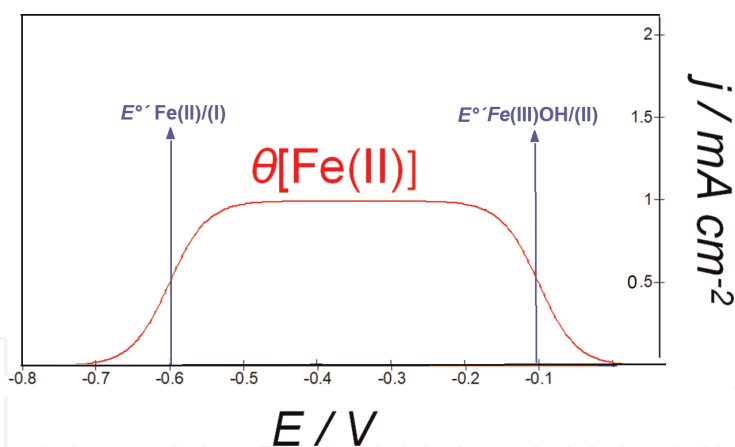


Figure 10. Mathematical simulation of the variation of fractional coverage $\theta_{Fe(II)}$ on the electrode surface as a function of potential for two hypothetical values of $E_{Fe(II)/(I)}$ and $E_{Fe(III)OH/(II)}$. Simulation involved the Nernst equation applied to surface confined species, assuming ideal behaviour (adapted from [26]).

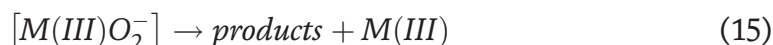
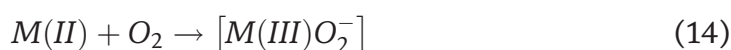
FePc in the oxidation state (II) simulated using Eq. (13). This profile is obtained by simply using the Nernst equation for adsorbed species. This figure can explain the decrease in catalytic activity at potentials below the $E_{Fe(II)/(I)}^{\circ}$ transition as it appears that Fe(I) is not such a good catalyst as Fe(II) and the selectivity of the reaction changes from four electrons to two electrons to give peroxide. That could explain the decline in the ORR currents at more negative potentials. For simplicity in Eq. (13), the concentration of OH^{-} was taken as unity:

$$\theta(Fe(II)) = \frac{\exp\left(\frac{F}{RT}(E - E_{II/I}^{\circ})\right)}{\left[1 + \exp\left(\frac{F}{RT}(E - E_{II/I}^{\circ})\right)\right]} \frac{1}{\left[1 + \exp\left(\frac{F}{RT}(E - E_{III/II}^{\circ})\right)\right]} \quad (13)$$

2.1.2.1 Effect of redox potential on the electrocatalytic activity of MN4 complexes for ORR

The catalytic properties of MN4 macrocyclics for ORR have been reviewed by many authors [1, 6, 12–16, 18, 19, 23, 25, 27, 28]. Catalytic activity and stability can also be improved by heat treatment of these complexes combined on carbon. The amount of literature on this topic is very large and is beyond the scope of this manuscript to discuss it in any detail. As pointed out above, there are several reviews on this subject [6, 18, 23, 29–31], so discussion will be focused on using the complex redox potential as a reactivity descriptor.

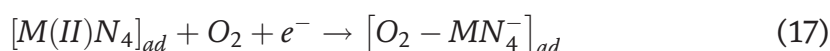
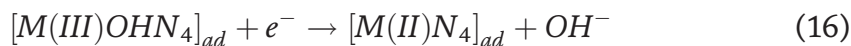
Randin was the first to attempt to rationalize the catalytic activity of MN4 complexes [32] in 1974 later followed by Beck in 1977 [33] using simply the redox potential of the MN4 complex as a reactivity indicator. A first theoretical explanation based on these terms was provided by Ulstrup in 1977 [34]. According to Randin and Beck, during the binding of O_2 to the metal ion in the complex, the metal is partially oxidized, thereby reducing the O_2 molecule according to the:



In order to account for supplementary experimental evidence, a somewhat modified model was proposed by Beck in which the central metal ion might also be only partially oxidized. According to reactions in Eqs. (14) and (15), the potential at

which O_2 is reduced should be closely related to the M(III)/M(II) redox potential of the central metal ion. Later studies published by van Veen et al. [23] using measurements of the redox potential of the complex under the same conditions as those under which the ORR kinetic data were obtained showed for the first time that the activity of several metal complexes, plotted as $\log i$ at constant potential versus the M(III)/(II) redox potential of the catalyst, gave a volcano-shaped curve (**Figure 7**).

More recent results comparing the activity of a large collection of MN₄ catalysts for ORR in alkaline media is shown in **Figure 8**. The data was reported by Zagal and Koper [6]. The volcano correlation illustrated in **Figure 8** shows two features. On the weak binding side, the two-electron reduction catalysts appear. According to the Sabatier principle for maximum catalytic activity, the binding of the reacting molecule needs to be not too strong and not too weak and to essentially explain the shape of the correlation where low activity is observed for low M-O₂ binding and for high M-O₂ binding energies. The highest activity is achieved for intermediate M-O₂ binding energies. The shape of the volcano correlation can also be explained using a Langmuir isotherm that essentially defines the coverage (θ) of M-O₂ species on the catalytic surface. Catalysts binding O_2 very weakly give very low values of θ and low activities, and the opposite is true for catalysts binding O_2 very strongly which give values of θ approaching unity, and in that case practically all the surface is occupied with adsorbed intermediates, blocking the active sites and again giving very low activities. These two extreme cases represent the foothills of both sides of the volcano correlation. It can be demonstrated that under standard conditions, the apex of the volcano corresponds to a situation where $\theta = 0.5$ and $\Delta G^\circ_{O_2} = 0$. For simplicity we consider the binding of O_2 to the active sites occurring with the transfer of a first electron, Eq. (17). This is generally the bottleneck of the whole reduction process leading to peroxide (two-electron transfers) or to water (four-electron transfer):



Depending on the catalyst, this equation will be shifted to the product (strong adsorption) or to the reactants (weak adsorption). Other adsorption steps can occur, involving other intermediates. The kinetic current density for a given potential consistent with the Butler-Volmer equation is given by the following equation neglecting the back reaction:

$$i = nFk \theta_{M(II)} p_{O_2} (1 - \theta) \exp^{-\beta FE/RT} \exp^{-\beta' \Delta G^\circ_{ad}/RT} \quad (18)$$

where β is the symmetry factor of the energy barrier and β' the is the Brönsted-Polanyi coefficient. β and β' can be assumed to be 0.5.

From the data in **Figure 8** we can assume that $\Delta G^\circ_{ad} = nFE^\circ + C$, where E° is the M(III)/(II) formal potential of each complex. The surface coverage of active sites varies as $0 < \theta_{M(II)} < 1$ depending on the electrode potential. **Figure 10** shows a simulation of the variation of $\theta_{M(II)}$ with potential using the Nernst equation for adsorbed species [26].

However, in the case of metal complexes with very negative redox potentials, the Fe(III)/Fe(II) redox transition also comes into play, lowering the fraction of catalytically active sites $\theta[M(II)]$ as illustrated in **Figure 10**. The M(II) active sites will predominate in the potential range, $E^{\circ'}_{(II/I)} \leq E \leq E^{\circ'}_{(III/II)}$, as illustrated in **Figure 10**.

Since the Fe(III) binds OH^- [35], these sites will be inactive for the reduction of O_2 ; the coverage of adsorbed O_2 can be assumed to follow a Langmuir isotherm:

$$\theta = \frac{p_{\text{O}_2} \exp(-\Delta G^\circ_{\text{O}_2}/RT)}{[1 + p_{\text{O}_2} \exp(-\Delta G^\circ_{\text{O}_2}/RT)]} \quad (19)$$

In volcano plots, the data for different catalysts is compared at constant E , so the Butler-Volmer exponential term for simplicity can be absorbed into the constant k' . For small coverages, $\Delta G^\circ_{\text{O}_2}$ is positive so Eq. (19) can be written as:

$$k' = k \exp(-\beta FE/RT) \quad (20)$$

$$i = nFk' \theta_{\text{M(II)}} p_{\text{O}_2} (1 - \theta_{\text{ad}}) \exp(-\beta' \Delta G^\circ_{\text{ad}}/RT) \quad (21)$$

$$(1 - \theta) = \frac{1 + p_{\text{O}_2} \exp(-\Delta G^\circ_{\text{O}_2}/RT)}{[1 + p_{\text{O}_2} \exp(-\Delta G^\circ_{\text{O}_2}/RT)]} - \frac{p_{\text{O}_2} \exp(-\Delta G^\circ_{\text{O}_2}/RT)}{1 + p_{\text{O}_2} \exp(-\Delta G^\circ_{\text{O}_2}/RT)} \quad (22)$$

$$(1 - \theta) = \frac{1}{[1 + p_{\text{O}_2} \exp(-\Delta G^\circ_{\text{O}_2}/RT)]} \quad (23)$$

$$i = \theta_{\text{Fe(II)}} \frac{nFk' p_{\text{O}_2} \exp(-\beta' \Delta G^\circ_{\text{O}_2}/RT)}{[1 + p_{\text{O}_2} \exp(-\Delta G^\circ_{\text{O}_2}/RT)]} \quad (24)$$

Equation (24) essentially describes the shape of the volcano plot of $\log i$ vs. $\Delta G^\circ_{\text{O}_2}$ and that the maximum current density will be observed for $\Delta G^\circ_{\text{O}_2} = 0$, and the maximum current at the apex of the volcano is:

$$i = \frac{nFk' \theta_{\text{Fe(II)}} p_{\text{O}_2}}{[1 + p_{\text{O}_2}]} \quad (25)$$

For strong adsorption, $\Delta G^\circ_{\text{O}_2}$ is large with a negative sign so $1 \ll p_{\text{O}_2} \exp(-\Delta G^\circ_{\text{O}_2}/RT)$, so the general Eq. (25) becomes:

Strong adsorption:

$$i = nFk' \Gamma \theta_{\text{Fe(II)}} \exp(+\beta' \Delta G^\circ_{\text{O}_2}/RT) \quad (26)$$

Equation (26) explains the linear correlation in the region of strong adsorption ($\Delta G^\circ_{\text{O}_2}$ is negative) and is essentially independent of the concentration of the reactant, in this case, O_2 .

For weak adsorption, $\Delta G^\circ_{\text{O}_2}$ is very positive, the term $p_{\text{O}_2} \exp(-\Delta G^\circ_{\text{O}_2}/RT) \ll 1$ in Eq. (24) vanishes, and the general Eq. (24) becomes simply:

Weak adsorption:

$$i = nFk' \theta_{\text{Fe(II)}} p_{\text{O}_2} \exp(-\beta' \Delta G^\circ_{\text{ad}}/RT) \quad (27)$$

So, Eqs. (26) and (27) describe both linear correlations in the volcano plots with slopes of different signs, i.e. $+\beta'/RT$ for the strong adsorption region and $-\beta' \Delta G^\circ_{\text{O}_2}/RT$ for the weak adsorption region. According to this, the volcano plot should be symmetrical since both legs of the volcano have the same absolute value of the slope. It is necessary to clarify that in theoretical calculations, the binding energy ΔE_{bO_2} is used because it does not contain entropy terms as $\Delta G^\circ_{\text{O}_2}$ and the entropic terms are difficult to estimate. The binding energy is essentially the energy to break the M- O_2 bond. If we use $\Delta G^\circ_{\text{ad}} = nFE^\circ + C$ and replacing the formula described above, the constant "C" can be adsorbed in a new constant k' :

Strong adsorption:

$$i = nFk''\theta_{M(II)} \exp\left(+\beta'E^\circ_{Fe(III)(II)}F/RT\right) \quad (28)$$

Weak adsorption:

$$i = nFk''\theta_{M(II)} p_{O_2} \exp\left(-\beta'E^\circ_{Fe(III)(II)}F/RT\right) \quad (29)$$

It is important to point out that β is the symmetry factor of the electron transfer energy barrier and β' is a Brönsted-Polanyi factor that reflects the effect of the adsorption on the activation energy. Both Eqs. (28) and (29) predict that the currents increase from positive E° (weak adsorption) to negative (strong adsorption) values of E° but up to 1 point. The highest activity will be at the intersection of those two lines. As the fraction of adsorbed intermediates θ increases, the currents start to decrease. This originates the “falling” side of the volcano, and the term $(1-\theta)$ tends to zero as $\theta \rightarrow 1$. This corresponds to the left side of the volcano correlation in **Figure 8**.

There is an alternative and more realistic explanation for the falling of the currents in the so-called “strong adsorption region”. Complexes located in that particular region are not necessarily in the M(II) active state. These complexes present Fe(III)/(II) redox potentials that are more negative than the electrode potentials used for comparing the activity. In those cases $\theta_{Fe(II)}$ can be lower than 1.

If we consider just the Fe(III)/(II) couple, as E is well above the $E^\circ_{Fe(II)/(I)}$ redox potential, we can use the Nernst equation for adsorbed species:

$$\theta_{Fe(II)} = \frac{1}{1 + \exp\left(\frac{F(E-E^\circ)}{RT}\right)} \quad (30)$$

where, for simplicity $E^\circ = E^\circ_{Fe(III)/(II)}$, $\theta_{Fe(II)}$ will become gradually smaller as $E \gg E^\circ_{Fe(III)/(II)}$. Eq. 30 carries the assumption that the adsorbed MN4 species behave ideally.

So if we consider that the falling region of the volcano correlation is attributed primarily to a gradual decrease in $\theta_{Fe(II)}$ and not to a gradual decrease in $(1-\theta)$, the amount of active sites is not then blocked by adsorbed intermediates. We can then introduce $\theta_{Fe(II)}$ in Eq. (31):

$$i = nFk''\theta_{M(II)} p_{O_2} \exp\left(-\beta'E^\circ F/RT\right) \quad (31)$$

$$i = \frac{nFk''M(II)p_{O_2} \exp\left(-\beta'E^\circ F/RT\right)}{1 + \exp\left(\frac{F(E-E^\circ)}{RT}\right)} \quad (32)$$

For those catalysts that have formal potentials below the electrode potential, $E^\circ \ll E \exp F/RT(E-E^\circ) \gg 1$, then the equation becomes:

$$i = nFk''p_{O_2} \exp\left[(-\beta'E^\circ F/RT) - ((EF/RT) - (E^\circ F/RT))\right] \quad (33)$$

$$i = nFk''p_{O_2} \exp\left[+(\beta'(E^\circ - E)F)/RT\right] \quad (34)$$

Equation (34) predicts that in the falling region of the volcano correlation, hypothetically the region of strong adsorption, the plot of $(\log i)_E$ versus E° should be linear with a slope of $+RT/\beta'F$. Assuming $\beta' = 0.5$ then the slope should be $+0.120$ V/decade which is close to the experimental value of $+0.140$ V/decade.

The gradual decrease in the currents on the falling region can then be attributed to the gradual decrease in $\theta_{Fe(II)}$ as the potential becomes more negative which somehow resembles what happens on metal electrodes where the surface becomes gradually covered with adsorbed intermediates. The volcano correlation where currents have been corrected for $\theta_{Fe(II)}$ becomes a linear correlation where the activity as $\log i$ increases with the driving force of the catalyst (see linear correlation in **Figure 11**). The slope is close to -0.120 V/decade again, very similar to the experimental value

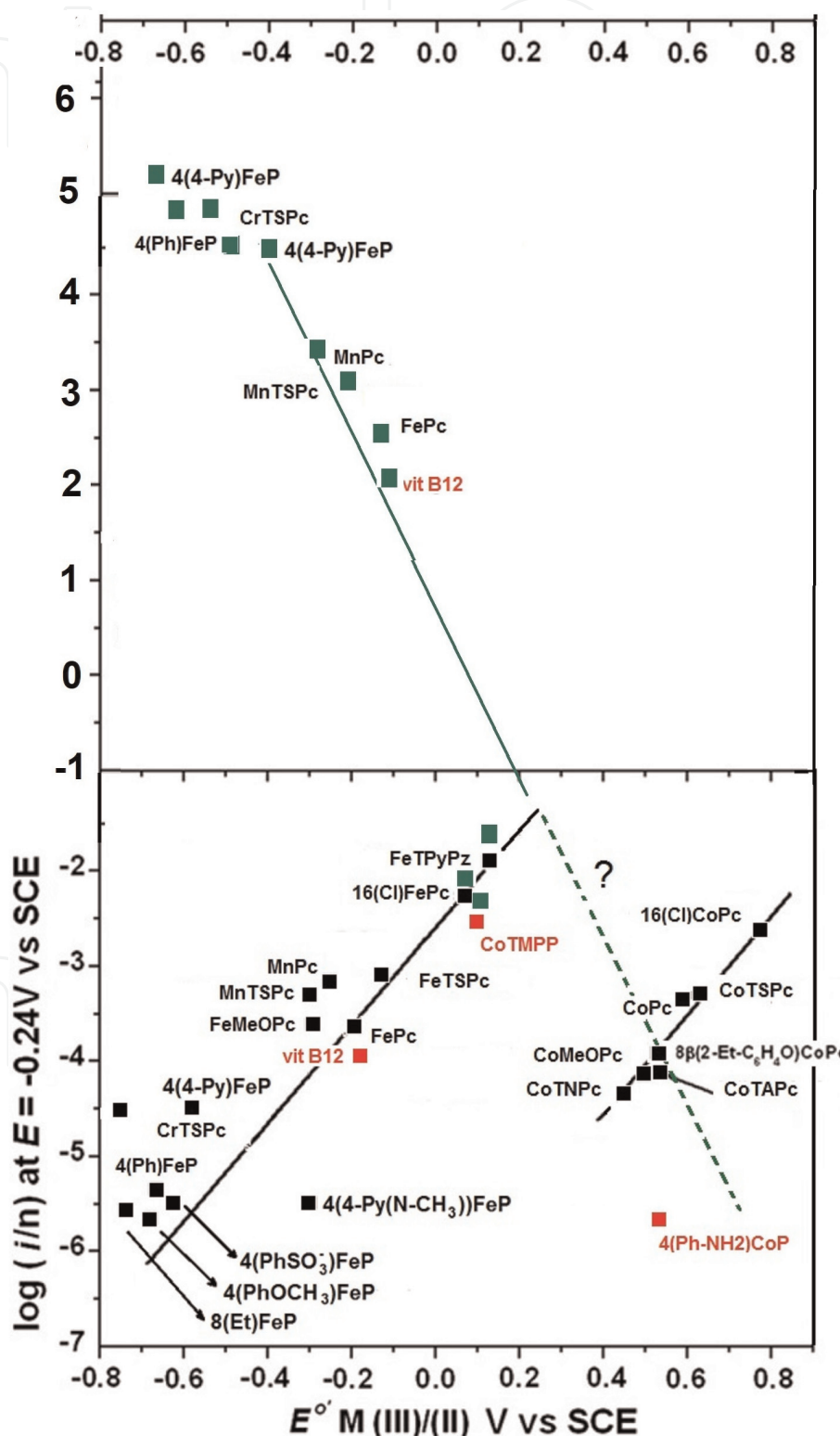


Figure 11. Volcano correlation of $\log(i/n)_E$ ($n = 4$ for Mn and Fe complexes and $n = 2$ for Co complexes, except vitamin B12) versus $E_{M(III)/(II)}$ for ORR. The linear correlation involves currents corrected for $\theta_{M(II)}$ as $\log(i/\theta_{M(II)} n)_E$. The only complexes affected are those having $E_{M(III)/(II)} < E$ (adapted from [6]).

of -0.130 V/decade. This also suggests that the redox potential of the catalysts acts as the driving force of the reaction, in a similar way of the electrode potential. The slope of this correlation is a linear free-energy correlation similar to a Tafel line where the driving force is provided by the overpotential. In inner-sphere chemical catalysis or electrocatalysis, the reacting molecule, in this case O_2 , does react promoted by two independent parameters: the electrode potential and the redox potential of the catalyst. The redox potential of the catalyst represents an excellent reactivity descriptor as it can be measured under the same conditions of the kinetic experiments. It is important to point out that the reactivity guidelines provided by MN4 macrocyclic complexes are also valid for smaller complexes like Cu phenanthrolines where the activity also depends in this case on the Cu(II)/(I) redox potential where the active state is Cu(I). For these complexes the activity of $(\log i)_E$ increases with the Cu(II)/(I) redox potential according to a linear correlation with a slope close to $+0.120$ V/decade. No volcano correlation is observed in this case. Since the slope has a positive sign, the correlation might correspond to the strong adsorption region, but this is not the case since calculated Cu- O_2 binding energies increase with the redox potential. In contrast to metal phthalocyanines and metal porphyrins, $\theta_{Cu(I)}$ is practically constant and equal to 1 since kinetic measurements were conducted at potentials well below the Cu(II)/(I) formal potentials of the catalysts examined. This will be discussed in detail in section 2.1.2.3.

Figure 12 shows a correlation for a series of Mn porphyrins for ORR versus the Mn(III)/(II) redox potential of the complexes. Again, the correlation has the shape of a volcano. Since as a parameter of activity the half-wave potential was used, it is difficult to estimate if the falling region is attributed to a damping effect of $\theta_{Mn(II)}$. However, the values of $E_{1/2}$ are well above the redox potential of the complexes.

2.1.2.2 Pyrolysed catalysts for ORR

As pointed out above, intact molecular catalysts like the metal complexes described above are not stable in fuel cell electrolytes so a whole new area of research started in the 1970s. The aim was to obtain pyrolytic materials from heat-treated MN4 complexes or other ingredients involving metal salts and carbon- and nitrogen-containing compounds [18, 29–31, 36–38]. Heat treatments of up to 1000° C have been used, and the structure of the obtained catalysts is still a matter of

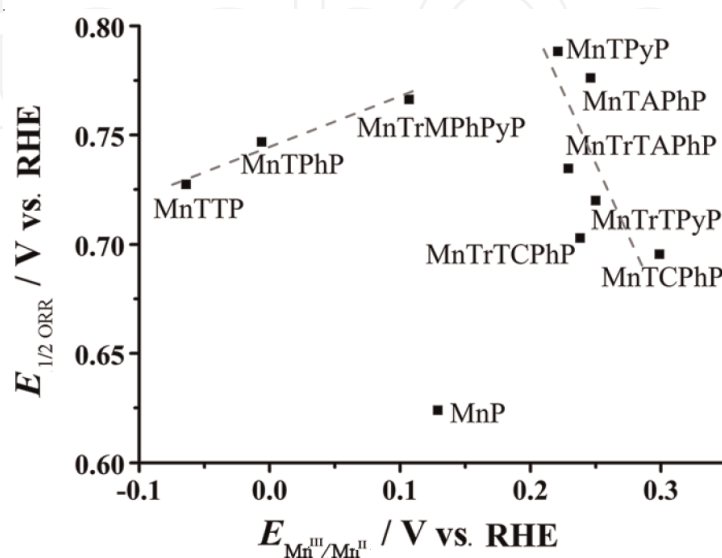


Figure 12. Volcano correlation of half-wave potential $E_{1/2}$ ORR versus the $E_{Mn(III)/(II)}$ [19] (reproduced by permission of Wiley).

debate. These materials are not only more stable but importantly also more active. The effects of the heat treatment on the activity were interpreted by van Veen et al. in terms of the M(III)/(II) redox potential [29, 30]. For example, when Fe porphyrins are pyrolysed, the ligand is destroyed by the pyrolysis, and the resulting surrounding ligand is much more electron-withdrawing in character. This results in a dramatic shift in the Fe(III)/(II) redox potential to more positive values. Literally, with heat treatment, the catalyst climbs the volcano correlation towards the top. Catalysts prepared without using a MN₄ complex but other ingredients also exhibit more positive redox potentials than intact metal complexes. Many very highly active pyrolysed MN_x catalysts do not exhibit visible redox signals in cyclic voltammograms, especially those prepared at higher temperatures, so the redox potential as predictor is lost. This could be attributed to the heterogeneity of active sites that can be formed at higher temperatures. Many authors have studied the changes occurring in carbon-supported metalloporphyrins and metallo-phthalocyanines. A variety of physical techniques have been used including X-ray photoelectron spectroscopy (XPS), Fourier-transform infrared spectroscopy, electron spin resonance and Mössbauer spectrometry and EXAFS [30].

When comparing the catalytic activity of a series of pyrolysed catalysts reported versus the M(III)/(II) redox potential, linear correlations are obtained which might correspond to incomplete volcano correlations (**Figure 13**) [39]. The slope is again +0.120 V/decade indicating that the equations derived above do explain both the experimental data of intact MN₄ catalysts and pyrolysed catalysts showing once more that the redox potential is a rather universal reactivity descriptor for ORR and

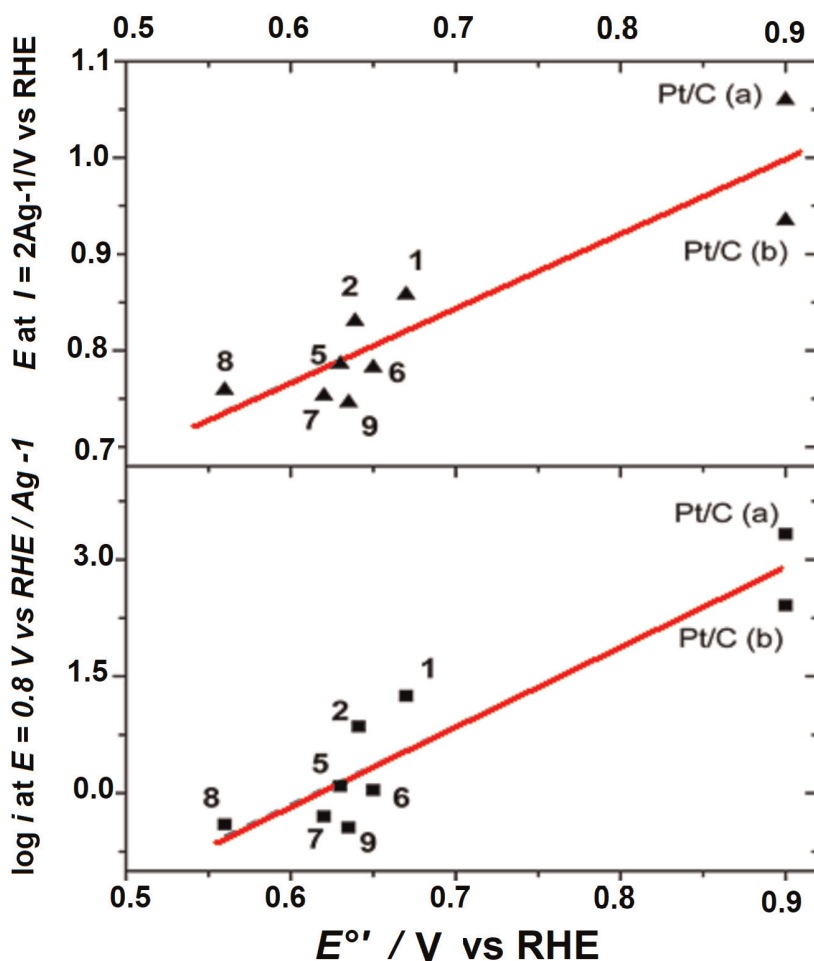


Figure 13. Linear correlations of E at constant current and $(\log i)_E$ versus $E_{M(III)/(II)}$ for a series of pyrolysed MN_x catalyst for ORR in acid media [39] (reproduced by permission of The Electrochemical Society).

possibly for other reactions [12, 13, 26]. The literature in this subject is very abundant, and more details and discussion about this pyrolysed MN_x catalysts are beyond the scope of this chapter. However, it is important to remark that the redox potential is a reactivity predictor for this very important family of catalysts.

2.1.2.3 Cu non-macrocyclic complexes

In nature copper-containing laccase is an enzyme that under certain conditions can promote the four-electron reduction of O₂ to water without the formation of any peroxide. Laccase only works at a very narrow pH range, and its large molecular size prevents high current densities. The reaction can occur at very low overpotentials, and this is indeed very unusual in ORR catalysts. For this reason, some authors [40–43] have explored the catalytic activity for ORR of simpler Cu complexes. For copper complexes, the active state is Cu(I). We will focus our discussion on the effect of the redox potential. The reactivity trends of metal phthalocyanines and metal porphyrins illustrated in **Figures 5** and **6** show that CuN₄ complexes exhibit very low activity for ORR. One of the reason for the low activity is that these Cu complexes are in the oxidation state Cu(II) and cannot be reduced to Cu(I) due to the rigidity of the planar phthalocyanine ligand since the reduction process involves a change in geometry around the Cu centre from planar Cu(II) to tetrahedral (Cu(I) (see **Figure 14**). The other reason is that CuPc has no frontier orbital with *d*-metal character that can bind O₂. This was illustrated in

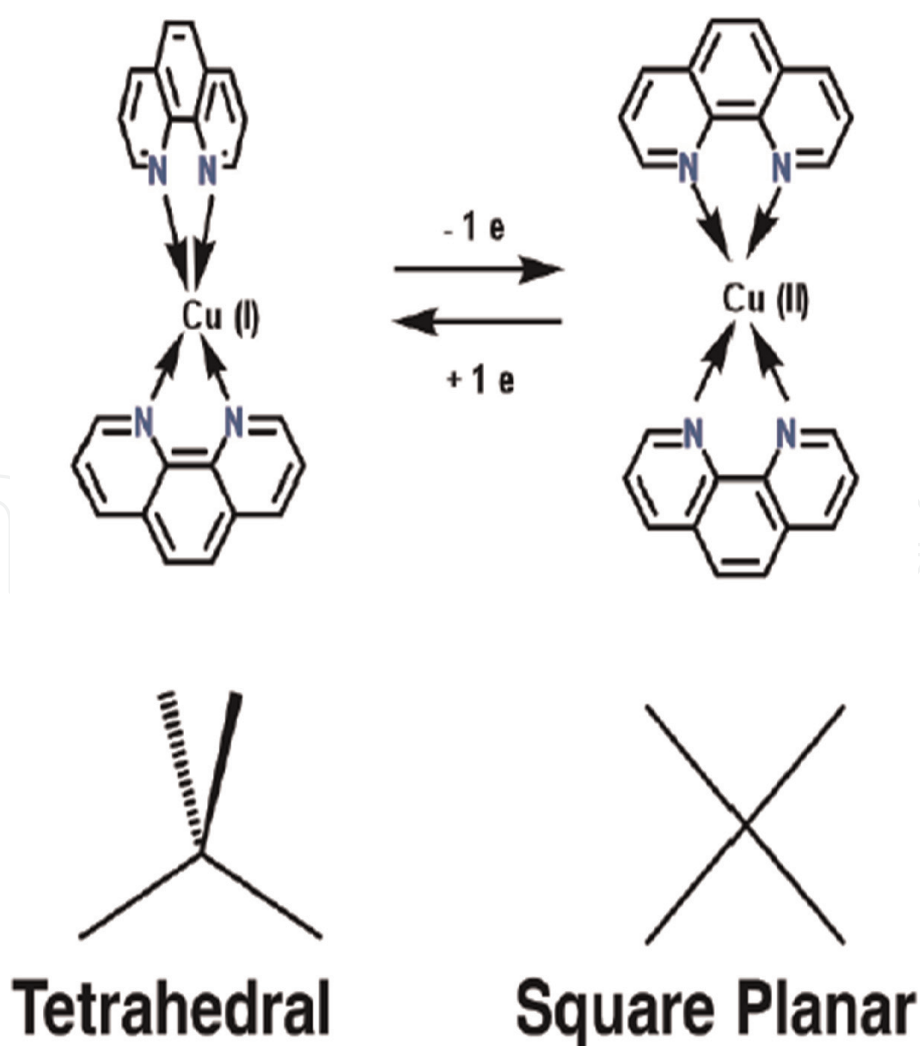


Figure 14. Illustration of changes in geometry when Cu(I) is oxidized to Cu(II) in a Cu(phen)₂ complex.

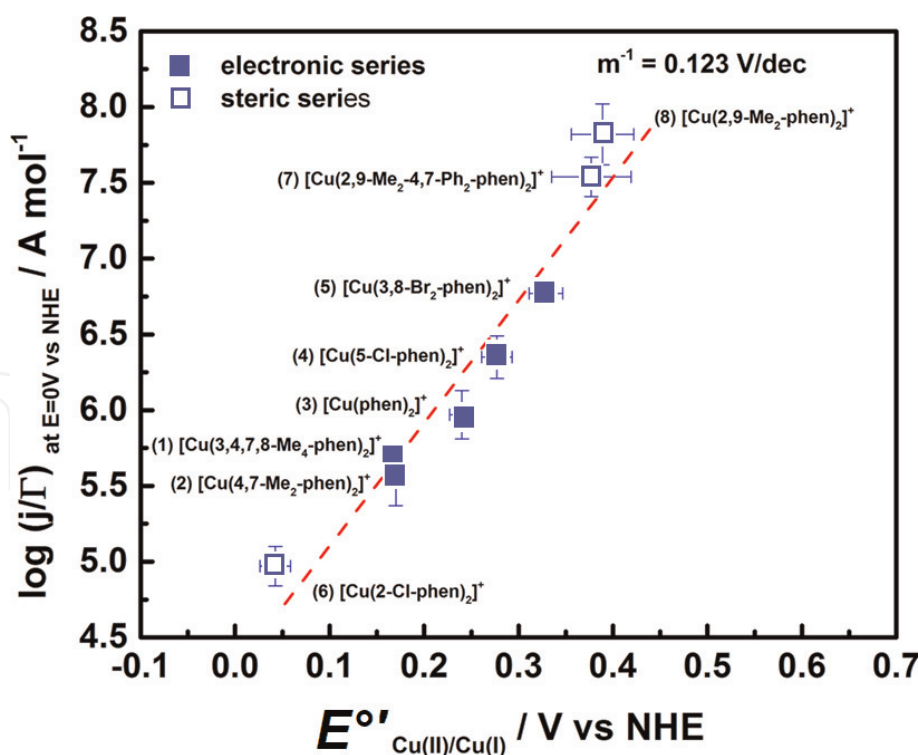


Figure 15. Plot of $\log(i/\Gamma)$ at $E = 0.0$ V vs. NHE versus the Cu(II)/(I) redox potential of the complex for ORR [44] (reproduced by permission of the American Chemical Society).

Figure 6. Cu phenanthrolines are flexible, and then redox processes can occur on the metal centre.

The Cu(II)/(I) redox potential of copper phenanthroline is a reactivity descriptor for ORR. **Figure 15** shows a linear correlation between $\log i$ and E° with a slope close to +0.120 V/decade which seems to be an incomplete volcano correlation [44].

3. Conclusions

The redox potential of the catalyst plays different roles in electrochemistry. Depending on whether the catalyst is present in the homogeneous phase or anchored or adsorbed on the electrode surface, the correlations between activity and redox potential can be different. For outer-sphere reactions occurring in the solution phase, the catalytic activity as $\log k$ versus the redox potential of the catalyst E° increases linearly with the redox potential, whereas for inner-sphere chemical catalysts, the activities observed are higher than those predicted by the redox potential of the catalyst.

For reactions promoted by molecular catalysts immobilized on the electrode surface, correlations of $(\log i)_E$ versus E° are observed. Linear and volcano correlations are obtained. When comparing MN4 macrocyclic complexes having a wide range of redox potentials, typical volcano correlations are generally observed in electrocatalysis. In classical volcano correlations, the different electrodes are metals or alloys. In this case the binding energy of key intermediates is used as reactivity descriptor. The activity gradually increases with the binding energy up to a point. Beyond that point the activity decreases with larger binding energies as the surface becomes covered with adsorbed intermediates. Similar correlations are observed with MN4 molecular catalysts. Further, with both metals and molecular catalysts, the strong adsorption region of the volcano involves the four-electron reduction of O_2 , whereas the weak adsorption region includes the two-electron reduction

catalysts. The decrease in activity for ORR using MN4 metal complexes does not seem to be related to a gradual occupation of the active site but rather to a gradual decrease in the amount of M(II) active sites. This is observed for those catalysts that have M(III)/(II) redox potentials more negative than the electrode potential chosen for comparing the activities. Cu phenanthroline complexes follow similar correlations. It is observed that the activity increases as the Cu(II)/(I) redox potential increases, showing only a linear correlation.

A general conclusion from electrocatalytic phenomena is that if volcano correlations are well established, then for a particular reaction the properties of the catalyst can be “tuned” so to improve their activity. The optimal properties can involve many other parameters such as metal-to-metal separation, crystal orientation, stability, alloying, nanostructure and redox potential of catalyst, so this is an open field for both experimentalists and theoreticians to find the ways of improving the catalytic activity of electrode surfaces.

The implications of future development in this area will have a tremendous impact in energy conversion devices, electrosynthesis and electrochemical sensors, just to mention a few.

Acknowledgements


This work has been financed by the Fondecyt Project 1181037, Fondecyt Project 1171408 and 1140199 and Núcleo Milenio de Ingeniería Molecular P07-006.

Author details

José H. Zagal*, Ingrid Ponce and Ruben Oñate
Department de Chemistry of Materials, Department of Chemistry of the Environment, Faculty of Chemistry and Biology, Laboratory of Electrocatalysis, University of Santiago de Chile, Santiago, Chile

*Address all correspondence to: jose.zagal@usach.cl

IntechOpen

© 2019 The Author(s). Licensee IntechOpen. This chapter is distributed under the terms of the Creative Commons Attribution License (<http://creativecommons.org/licenses/by/3.0>), which permits unrestricted use, distribution, and reproduction in any medium, provided the original work is properly cited. 

References

- [1] Appleby AJ, Zagal JH. Free energy relationships in electrochemistry: A history that started in 1935. *Journal of Solid State Electrochemistry*. 2011;**15**: 1811-1832. DOI: 10.1007/s10008-011-1394-8
- [2] Frumkin A. Bemerkung zur Theorie der Wasserstoffüberspannung. *Zeitschrift für Physikalische Chemie*. 1932;**160A**:116-118. DOI: 10.1515/zpch-1932-16011
- [3] Bockris JO, Khan SUM. Some experimental techniques. In: *Surface Electrochemistry*. Boston, MA: Springer US; 1993. pp. 1-58. DOI: 10.1007/978-1-4615-3040-4_1
- [4] Tafel J. Über die Polarisation bei kathodischer Wasserstoffentwicklung. *Zeitschrift für Physikalische Chemie*. 1905;**50**:641-712. DOI: 10.1515/zpch-1905-5043
- [5] Petrii OA, Nazmutdinov RR, Bronshtein MD, Tsirlina GA. Life of the Tafel equation: Current understanding and prospects for the second century. *Electrochimica Acta*. 2007;**52**: 3493-3504. DOI: 10.1016/j.electacta.2006.10.014
- [6] Zagal JH, Koper MTM. Reactivity descriptors for the activity of molecular MN₄ catalysts for the oxygen reduction reaction. *Angew Chemie*. 2016;**55**: 14510-14521. DOI: 10.1002/anie.201604311
- [7] Savéant J-M. *Elements of Molecular and Biomolecular Electrochemistry*. Hoboken, NJ, USA: John Wiley & Sons, Inc.; 2006. DOI: 10.1002/0471758078
- [8] Lexa D, Mispelter J, Savéant JM. Electroreductive alkylation of iron in porphyrin complexes. Electrochemical and spectral characteristics of Sigma-alkylironporphyrins. *Journal of the American Chemical Society*. 1981;**103**: 6806-6812. DOI: 10.1021/ja00413a004
- [9] Lexa D, Savéant JM, Wang DL. Electroreductive alkylation of iron porphyrins. Iron(III), iron(II) and iron (I) alkyl complexes from the reaction of doubly reduced iron(II) porphyrins with alkyl halides. *Organometallics*. 1986;**5**:1428-1434. DOI: 10.1021/om00138a022
- [10] Lexa D, Savéant JM, Su KB, Wang DL. Chemical vs. redox catalysis of electrochemical reactions. Reduction of trans-1,2-dibromocyclohexane by electrogenerated aromatic anion radicals and low oxidation state metalloporphyrins. *Journal of the American Chemical Society*. 1987;**109**: 6464-6470. DOI: 10.1021/ja00255a036
- [11] Lexa D, Savéant JM, Schaefer HJ, Khac Binh S, Vering B, Wang DL. Outer-sphere and inner-sphere processes in reductive elimination. Direct and indirect electrochemical reduction of vicinal dibromoalkanes. *Journal of the American Chemical Society*. 1990;**112**:6162-6177. DOI: 10.1021/ja00173a002
- [12] Zagal JH. Metallophthalocyanines as catalysts in electrochemical reactions. *Coordination Chemistry Reviews*. 1992;**119**:89-136. DOI: 10.1016/0010-8545(92)80031-L
- [13] Zagal JH, Griveau S, Silva JF, Nyokong T, Bedioui F. Metallophthalocyanine-based molecular materials as catalysts for electrochemical reactions. *Coordination Chemistry Reviews*. 2010;**254**: 2755-2791. DOI: 10.1016/j.ccr.2010.05.001
- [14] Masa J, Ozoemena K, Schuhmann W, Zagal JH. Oxygen reduction reaction using N₄ - metallomacrocyclic catalysts:

- Fundamentals on rational catalyst design. *Journal of Porphyrins and Phthalocyanines*. 2012;**16**:761-784. DOI: 10.1142/S1088424612300091
- [15] Boulatov R. Billion-year-old oxygen cathode that actually works: Respiratory oxygen reduction and its biomimetic analogs. In: Zagal JH, Bedioui F, Dodelet J-P, editors. *N4-Macrocyclic Metal Complexes*. New York, NY: Springer New York; 2006. pp. 1-40. DOI: 10.1007/978-0-387-28430-9_1
- [16] Zagal JH, Páez MA, Silva JF. Fundamental aspects on the catalytic activity of metallomacrocyclics for the electrochemical reduction of O₂. In: Zagal JH, Bedioui F, Dodelet J-P, editors. *N4-Macrocyclic Metal Complexes*. New York, NY: Springer New York; 2006. pp. 41-82. DOI: 10.1007/978-0-387-28430-9_2
- [17] Jasinski R. A new fuel cell cathode catalyst. *Nature*. 1964;**201**:1212-1213. DOI: 10.1038/2011212a0
- [18] Dodelet J-P. Oxygen reduction in PEM fuel cell conditions: Heat-treated non-precious metal-N₄ macrocycles and beyond. In: Zagal JH, Bedioui F, Dodelet J-P, editors. *N4-Macrocyclic Metal Complexes*. New York, NY: Springer New York; 2006. pp. 83-147. DOI: 10.1007/978-0-387-28430-9_3
- [19] Masa J, Schuhmann W. Systematic selection of metalloporphyrin-based catalysts for oxygen reduction by modulation of the donor-acceptor intermolecular hardness. *Chemistry: A European Journal*. 2013;**19**: 9644-9654. DOI: 10.1002/chem.201203846
- [20] Hipps KW, Lu X, Wang XD, Mazur U. Metal d-orbital occupation-dependent images in the scanning tunneling microscopy of metal phthalocyanines. *The Journal of Physical Chemistry*. 1996;**100**: 11207-11210. DOI: 10.1021/jp960422o
- [21] Wang Y, Wu K, Kröger J, Berndt R. Review article: Structures of phthalocyanine molecules on surfaces studied by STM. *AIP Advances*. 2012;**2**: 041402. DOI: 10.1063/1.4773458
- [22] Cárdenas-Jirón GI, Gulppi MA, Caro CA, del Río R, Páez M, Zagal JH. Reactivity of electrodes modified with substituted metallophthalocyanines. Correlations with redox potentials, Hammett parameters and donor-acceptor intermolecular hardness. *Electrochimica Acta*. 2001;**46**:3227-3235. DOI: 10.1016/S0013-4686(01)00614-4
- [23] van Veen JAR, van Baar JF, Kroese KJ. Effect of heat treatment on the performance of carbon-supported transition-metal chelates in the electrochemical reduction of oxygen. *Journal of the Chemical Society, Faraday Transactions*. 1981;**77**: 2827-2843. DOI: 10.1039/f19817702827
- [24] Nørskov JK, Rossmeisl J, Logadottir A, Lindqvist L, Kitchin JR, Bligaard T, et al. Origin of the overpotential for oxygen reduction at a fuel-cell cathode. *The Journal of Physical Chemistry. B*. 2004;**108**: 17886-17892. DOI: 10.1021/jp047349j
- [25] Zagal JH, Javier Recio F, Gutierrez CA, Zuñiga C, Páez MA, Caro CA. Towards a unified way of comparing the electrocatalytic activity MN₄ macrocyclic metal catalysts for O₂ reduction on the basis of the reversible potential of the reaction. *Electrochemistry Communications*. 2014;**41**:24-26. DOI: 10.1016/j.elecom.2014.01.009
- [26] Silva N, Calderón S, Páez MA, Oyarzún MP, Koper MTM, Zagal JH. Probing the Feⁿ⁺/Fe⁽ⁿ⁻¹⁾⁺ redox potential of Fe phthalocyanines and Fe porphyrins as a reactivity descriptor in the electrochemical oxidation of cysteamine. *Journal of Electroanalytical Chemistry*. 2018;**819**:502-510. DOI: 10.1016/J.JELECHEM.2017.12.068

- [27] Zagal JH, Aguirre MJ, Páez MA. O₂ reduction kinetics on a graphite electrode modified with adsorbed vitamin B12. *Journal of Electroanalytical Chemistry*. 1997;**437**:45-52. DOI: 10.1016/S0022-0728(97)00253-2
- [28] Cárdenas-Jirón GI, Zagal JH. Donor-acceptor intermolecular hardness on charge transfer reactions of substituted cobalt phthalocyanines. *Journal of Electroanalytical Chemistry*. 2001;**497**:55-60. DOI: 10.1016/S0022-0728(00)00434-4
- [29] van Veen JAR, Colijn HA, van Baar JF. On the effect of a heat treatment on the structure of carbon-supported metalloporphyrins and phthalocyanines. *Electrochimica Acta*. 1988;**33**:801-804. DOI: 10.1016/S0013-4686(98)80010-8
- [30] Bouwkamp-Wijnoltz AL, Visscher W, van Veen JAR, Boellaard E, van der Kraan AM, Tang SC. On active-site heterogeneity in pyrolyzed carbon-supported iron porphyrin catalysts for the electrochemical reduction of oxygen: An in situ Mössbauer study. *The Journal of Physical Chemistry. B*. 2002; **106**:12993-13001. DOI: 10.1021/jp0266087
- [31] Chen Z, Higgins D, Yu A, Zhang L, Zhang J. A review on non-precious metal electrocatalysts for PEM fuel cells. *Energy & Environmental Science*. 2011;**4**:3167. DOI: 10.1039/c0ee00558d
- [32] Randin J-P. Interpretation of the relative electrochemical activity of various metal phthalocyanines for the oxygen reduction reaction. *Electrochimica Acta*. 1974;**19**:83-85. DOI: 10.1016/0013-4686(74)85060-7
- [33] Beck F. The redox mechanism of the chelate-catalyzed oxygen cathode. *Journal of Applied Electrochemistry*. 1977;**7**:239-245. DOI: 10.1007/BF00618991
- [34] Ulstrup J. Catalysis of the electrochemical reduction of molecular oxygen by metal phthalocyanines. *Journal of Electroanalytical Chemistry*. 1977;**79**:191-197. DOI: 10.1016/S0022-0728(77)80411-7
- [35] Zagal JH, Gulppi M, Isaacs M, Cárdenas-Jirón G, Aguirre MJ. Linear versus volcano correlations between electrocatalytic activity and redox and electronic properties of metallophthalocyanines. *Electrochimica Acta*. 1998;**44**:1349-1357. DOI: 10.1016/S0013-4686(98)00257-6
- [36] Zhang L, Zhang J, Wilkinson DP, Wang H. Progress in preparation of non-noble electrocatalysts for PEM fuel cell reactions. *Journal of Power Sources*. 2006;**156**:171-182. DOI: 10.1016/J.JPOWSOUR.2005.05.069
- [37] Bezerra CWB, Zhang L, Liu H, Lee K, Marques ALB, Marques EP, et al. A review of heat-treatment effects on activity and stability of PEM fuel cell catalysts for oxygen reduction reaction. *Journal of Power Sources*. 2007;**173**: 891-908. DOI: 10.1016/J.JPOWSOUR.2007.08.028
- [38] Song C, Zhang J. Electrocatalytic oxygen reduction reaction. In: Zhang J, editor. *PEM Fuel Cell Electrocatalysts and Catalyst Layers*. London: Springer London; 2008. pp. 89-134. DOI: 10.1007/978-1-84800-936-3_2
- [39] Zagal JH, Ponce I, Baez D, Venegas R, Pavez J, Paez M, et al. A possible interpretation for the high catalytic activity of heat-treated non-precious metal Nx/C catalysts for O₂ reduction in terms of their formal reduction potentials. *Electrochemical and Solid-State Letters*. 2012;**15**:B90. DOI: 10.1149/2.032206esl
- [40] Thorseth MA, Tornow CE, Tse ECM, Gewirth AA. Cu complexes that catalyze the oxygen reduction reaction. *Coordination Chemistry*

Reviews. 2013;**257**:130-139. DOI:
10.1016/j.ccr.2012.03.033

[41] McCrory CCL, Ottenwaelder X, Stack TDP, Chidsey CED. Kinetic and mechanistic studies of the electrocatalytic reduction of O₂ to H₂O with mononuclear Cu complexes of substituted 1,10-phenanthrolines. *The Journal of Physical Chemistry. A.* 2007;**111**:12641-12650. DOI: 10.1021/jp076106z

[42] Solomon EI, Augustine AJ, Yoon J. O₂ reduction to H₂O by the multicopper oxidases. *Dalton Transactions.* 2008;**30**: 3921. DOI: 10.1039/b800799c

[43] Lei Y, Anson FC. Dynamics of the coordination equilibria in solutions containing copper(II), copper(I), and 2,9-dimethyl-1,10-phenanthroline and their effect on the reduction of O₂ by Cu (I). *Inorganic Chemistry.* 1995;**34**: 1083-1089. DOI: 10.1021/ic00109a014

[44] Venegas R, Muñoz-Becerra K, Lemus LA, Toro-Labbé A, Zagal JH, Recio FJ. Theoretical and experimental reactivity predictors for the electrocatalytic activity of copper phenanthroline derivatives for the reduction of dioxygen. *Journal of Physical Chemistry C.* 2019;**332**: 19468-19478. DOI: 10.1021/acs.jpcc.9b03200